CryoLetters 47(6), 414-424 (2026)
© CryoLetters, editor@cryoletters.org
https://doi.org/10.54680/fr26610110712

SUPERHYDROPHOBIC SOOT COATINGS-REGULATED CRYOSTORAGE OF HUMAN EJACULATE ENABLES EQUAL POST-THAW SPERM SURVIVAL INDEPENDENT OF THE FREEZING RATE

Karekin D. Esmeryan[1]* and Todor A. Chaushev[2]

[1] Acoustoelectronics Laboratory, Georgi Nadjakov Institute of Solid State Physics, Bulgarian Academy of Sciences, 72, Tzarigradsko Chaussee Blvd., 1784 Sofia, Bulgaria.
[2] Specialized Surgical Hospital "Doctor Malinov", 46, Gotse Delchev blvd., 1860 Sofia, Bulgaria.
Corresponding author's E-mail: karekin_esmerian@abv.bg

Abstract

BACKGROUND: In-vitro fertilization is a powerful technology contributing to the successful reproduction of the human race with over 13 million infants born since its launch in 1978. Yet, the pregnancy rate of this technique, when the underlying cause is male infertility, is low and reaches 10–45% per first attempt. It is often the case that embryologists utilize cryopreserved spermatozoa with declined post-thaw functionality due to multiple morphochemical alterations in semen inflicted by the freezing process. However, the era of molecular engineering provides measures to prevent cryodamage. **OBJECTIVE:** To explore the potential of superhydrophobic carbon soot to alleviate osmotic stress during the cryopreservation protocol. **RESULTS:** We reveal groundbreaking findings showing that the extremely water-repellent soot coatings, or the combination of submilliliter ejaculate volumes and hydrophilic interfaces, neutralize the effect of cooling velocity on the vitality and motility of thawed sperm. Hence, identical survival rates and, sometimes, percentage of forward-moving spermatozoa are observed after slow cooling (from +21 °C to -196 °C for 1200 s) or flash freezing (from +21 °C to -196 °C for ~4–20 s). **CONCLUSION:** The non-wettable soot functions as a thermal barrier managing the heat flux to compensate the dehydration of male gametes, while larger liquid volumes widen the inter-ice crystal distances, favoring cell recovery. Such an unexpected outcome reinforces the potential for developing standardized and methodology-independent techniques for sperm cryostorage, marking a crucial milestone in research conducted by the scientific community since the 1970s.

Keywords: cryoprotectant-free cryopreservation; human semen; instant freezing; soot.

INTRODUCTION

Complete preservation of progressive post-thaw sperm motility is a societal challenge linked to the increasing rate of male factor infertility, threatening human reproduction (1, 2, 3). Despite recent advancements in cryobiology, freezing-thawing cycles cause irreversible structural and functional injuries to spermatozoa related to osmotic stress (4, 5, 6).

The primary concern in cell cryopreservation is maintaining the biological suspension in an isotonic state (7), since exogeneous ice formation hyperconcentrates the surrounding solution, with some protection provided by the presence of anti-freeze agents in cytoplasm, such as proteins and sugars (8, 9). Extracellular crystallization changes osmotic equilibrium and induces exosmosis-driven dehydration (10, 11). If cooling is too slow and the water leakage rate fails to match that of extracellular ice growth, rheological deformation or solute-induced shock may occur (12). Very

rapid cooling, in contrast, impedes total cytoplasmic dehydration, causing intracellular icing that ruptures the cell membrane (11). Furthermore, fast freezing can also trigger partial vitrification of the extracellular medium and subsequent thawing is accompanied by massive water influx due to the high osmotic pressure, resulting in cytolysis (13). Neutralizing one of the mentioned adverse effects directly provokes the other – a systemic issue from the 1970s, known as the two-factor freezing injury (14).

Decades of research in cryobiology outline efficient approaches for mitigating the two-factor freezing injury risk by virtue of permeable cryoprotectants (15). They diffuse uniformly into the cytosol and extracellular compartment, thereby reducing ice accumulation, maintaining osmotic balance and increasing the volume of ice channels accommodating the cells (16, 17). If non-permeable, cryoprotectants enhance extracellular hyperosmolarity and regulate cellular dehydration and rehydration (18). Combined with permeable cryoprotective agents, this allows successful freezing-thawing of different sperm concentrations while preserving motility, acrosomes and DNA integrity (3, 19, 20, 21, 22). Despite their efficacy, permeable cryoprotectants are cytotoxic because of multiple cell volume fluctuations inflicted by slower than water membrane permeation (15). This necessitates minimizing their concentration and prompt, yet harmful, post-thaw removal (21). Although non-permeable solutes have low-level toxicity (18, 23), all current cryoprotocols result in an unavoidable decline in sperm motility (3, 19, 20, 21).

Embryologists may overcome the obstacles associated with cryostorage of human semen by fabricating superhydrophobic freezing containers internally coated with rapeseed oil soot. This nanomaterial mitigates cryoinjury by inhibiting ice formation and devitrification, and modulating osmotic water efflux, achieving up to 100% recovered sperm motility independently of the type of commercial cryoprotectants (24, 25, 26, 27). Key gaps hinder the transfer of soot-based cryopreservation methods to fertility clinics, primarily understanding whether carbon nanostructures negate the effect of freezing on sperm vitality, and whether such a method advances biobanking of human or animal ejaculates.

This study expands the frontier of knowledge in sperm cryostorage by identifying how the surface profile of superhydrophobic soot coatings affects the cryotolerance of human spermatozoa during flash freezing – a still-unexplored field. Comparing the results with those from slow freezing, we correlate the differences in cooling velocities with the morphochemical features of soot and the success of cryopreservation, aiming to achieve future optimal cryostasis for maximum post-thaw cell recovery in all cryogenic facilities. The newly presented data explain the probable reasons behind the similar survival rates across distinct freezing interfaces, cooling rates and liquid volumes – a unique outcome that shifts the paradigm in cryobiology.

MATERIALS AND METHODS

Materials

Valerus Ltd., Bulgaria, and Grangers International Ltd., United Kingdom, delivered ethanol (99 wt.%) and perfluorinated chemicals. Office1 Superstore, Bulgaria, provided paper napkins and cyanoacrylate glue, while crystalline silver hydrogen fluoride ($AgHF_2$) was purchased from Alfa Aesar, Germany. The synthesis of hydrophobic soot was performed by burning rapeseed oil, kindly supplied by Zoya Organic&Natural, Bulgaria.

Fabrication of five sheet metal cryoboxes coated with distinct water-repellent soot

To establish unequivocal correlations, the soot coatings included in this research were the same as those used for slow sperm freezing (26). Roughly 20–30 mL of rapeseed oil was poured over a vertical cylindrical paper wick situated in a metal Petri dish. It was then ignited and the whole construct was mounted inside a steel conical chimney, hosting the combustion. The atmospheric air was generated by a compressor and entered the reaction zone via a hose connected to a flow meter/controller maintaining an air flow rate of 0.0052 m^3/min. This engineering design enabled the synthesis of quasispherical-shaped soot nanoparticles deposited as a coating on a 25×25 mm sheet metal cryobox (27), immersed later in ethanol for 5 s, fluorocarbon suspension for 600 s and dried on a hot plate at 200 °C. Next, the air flow was decreased to 0.0032 m^3/min, transforming the soot into quasisquare carbon agglomerates

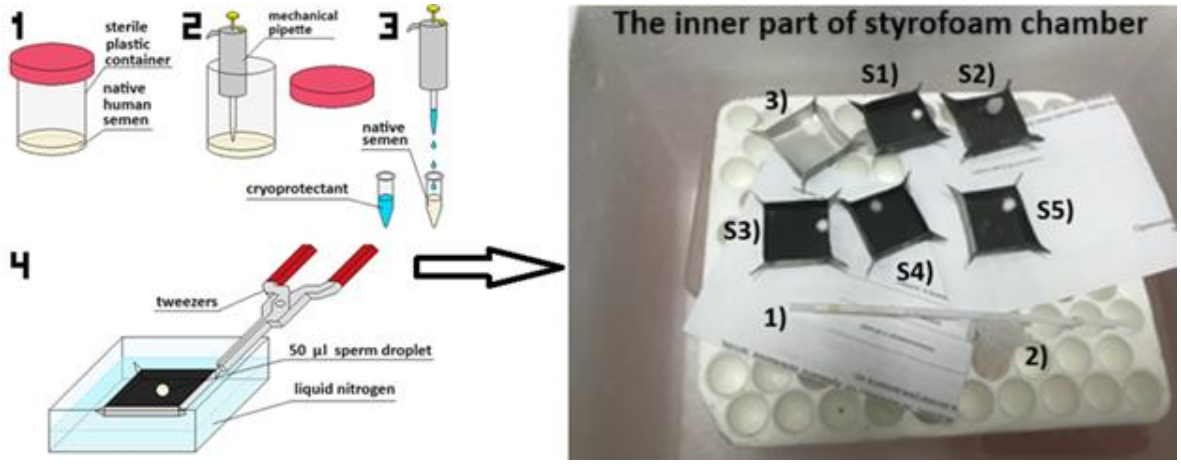


Figure 1. Experimental setup for flash freezing of human ejaculate. Nomenclature: 1) Straw – first control; 2) Cryovial – second control; 3) Uncoated sheet metal cryobox – third control; S1) – silver-doped soot; S2) soot fabrics; S3) quasisquare soot treated with ethanol and fluorocarbon; S4) pristine quasisquare soot; S5) quasispherical soot treated with ethanol and fluorocarbon. A standalone soot fabric membrane (sample S5 in ref. [26]) is excluded, because it cannot stably hold the sperm droplet upon immersion in liquid nitrogen (step 4 in Figure 1).

deposited on two new cryoboxes, one of which was left chemically untreated. Subsequently, a fourth cryobox was covered by double-sided sticky tape and a paper napkin, sooted for 30 s, soaked with ~210–230 mg of cyanoacrylate glue and immersed in 80% v/v perfluorocarbon aqueous solution (25, 27). A colloid composed of 50 mL ethanol, 500 mg quasispherical soot and 200 mg $AgHF_2$ was placed in a plastic atomizer, sonicated for 40 min and sprayed onto a fifth cryobox, heated to 200 °C, at nozzle-to-substrate distance of ~150 mm (26). These fabrication steps yilded five types of soot-coated cryoboxes useful for cryostorage.

Flash freezing and slow warming of human ejaculate via soot-coated cryoboxes

In order to properly interpret the obtained results, high-speed freezing of human semen via soot-coated cryoboxes was accomplished in several steps (Fig. 1). The seminal fluids of the same nine patients who previously participated in slow cooling tests (26) were used.

The fresh ejaculate of each volunteer was collected in a sterile plastic container and after 30 min liquefaction at 37 °C in an incubator, 10 µL of semen was placed in a Makler chamber and subjected to computer-assisted analysis via an SCA 6.0.0.2 Microptic S. L. software. Several areas were scanned until a minimum number of 500 spermatozoa were counted (when possible). Four hundred µL of Quinn's Advantage Sperm Freezing Medium (Cooper Surgical, USA) was mixed with 400 µL of liquefied seminal fluid by adding eight consecutive 50 µL droplets over a period of 240 s. The suspension was equilibrated for 180 s and the sperm concentration and motility were measured via the computer software (control values). Flash freezing was performed by taking a 50 µL droplet from the sperm-cryoprotectant soluton, placing it on a given soot-coated cryobox, immersing its bottom and sidewalls in a plastic tub filled with liquid nitrogen and recording the recalescent freezing time with a chronometer. The sample was then moved into a styrofoam chamber and exposed to liquid nitrogen vapour. This procedure was repeated for all cryoboxes, including an uncoated control specimen, a cryostraw and a cryovial filled with 100 µL and 400 µL semen-cryoprotectant mixture, respectively (two additional controls). After 60 min, the specimens were taken out one by one, thawed slowly at room temperature (T_{room} ~21 ±0.5 °C) and analyzed again for sperm parameters. This methodology provided insights into how the physicochemical profile and wettability of the freezing interface, solid-coolant contact area and liquid volume affect human spermatozoa survival during flash freezing. Note that slow, rather than fast, warming was implemented, as the soot appears

to impede devitrification and recrystallization upon thawing (26, 27). The hydrophilic cryostraw and cryovial were used to compare our approach with conventional methods for sperm cryostorage (20, 21). Cooling and warming rates were determined as described in ref. (27).

Informed consents were obtained to use the semen for research, in compliance with the license of Specialized Surgical Hospital "Doctor Malinov" for assisted reproduction activities (ref. № СБ-287/02.11.2021), and the studies conformed to the Declaration of Helsinki.

Statistical analysis

Statistical dispersion of the experimental results was performed by calculating their mean values and standard deviations using Microsoft Excel. Analysis of Variance (ANOVA) test was carried out with the same software to define the significance of statistical variations among the individual groups of data. P-values ≤ 0.05 were considered evidence against the null hypothesis.

RESULTS

Introduction to the physicochemical features of rapeseed oil soot

Figures 2 and 3 show scanning electron microscopy images of the five soot patterns deposited on the sheet metal cryoboxes.

The thermochemical decomposition of the vaporizing oil initiates the formation of polycyclic aromatic hydrocarbons. These compounds undergo bond breaking via a hydrogen abstraction mechanism, generating acetylene molecules that build up and grow into spherical carbonaceous particles, called soot (28). In the conical chimney, this occurs at an air flow of 0.0052 m^3/min. The deposited nanomaterial is characterized by a fractal-like structure composed of spherical particles with ~50 nm diameter, arranged into larger aggregates (see sample S5 in Fig. 3). Reducing the air flow to 0.0032 m^3/min altered the chemical kinetics of the combustion process, converting the soot into fused micron-sized quasisquare agglomerates (see samples S3-S4 in Figs 2 and 3). The alcohol treatment compacted the carbon nanostructures, increased their surface oxidation and altered the size of solid agglomerates (29). Thus, the total pore fraction, φ, and the median pore size, μ, of quasisquare

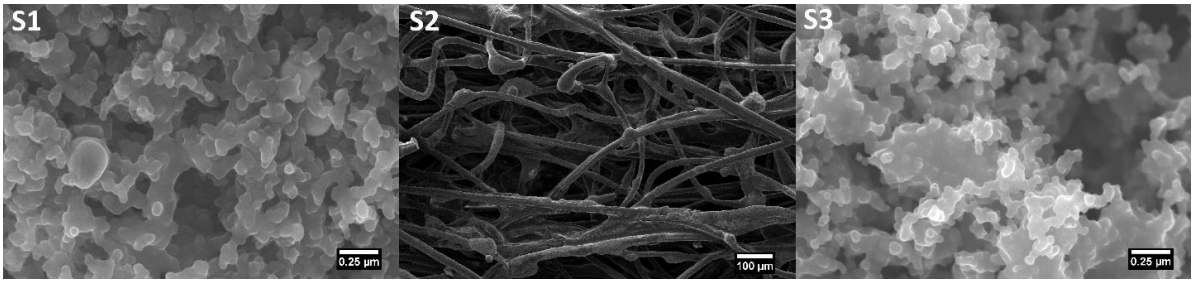


Figure 2. Shape and size of carbon nanostructures constituting the surfaces made of silver-doped soot (S1), soot fabrics (S2) and quasisquare soot treated with ethanol and fluorocarbon (S3).

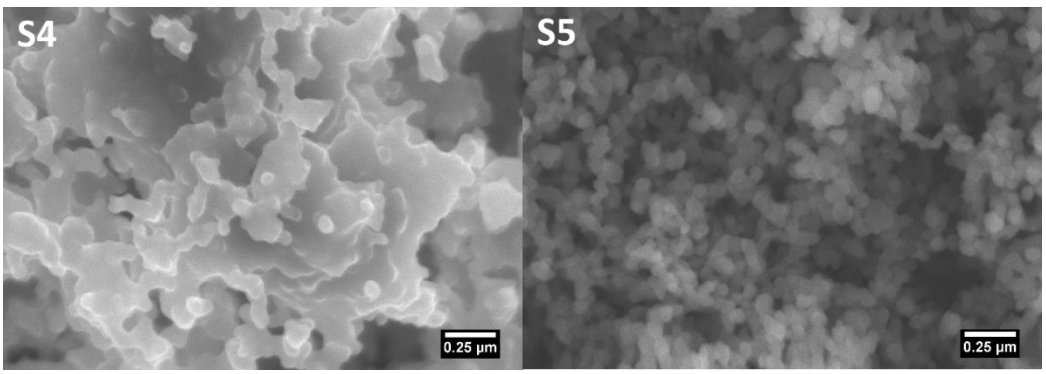


Figure 3. Shape and size of carbon nanostructures constituting the surfaces made of pristine quasisquare soot (S4) and quasispherical soot treated with ethanol and fluorocarbon (S5)

soot increased by 9% and 34%, while for the quasispherical counterpart, μ remains ~45 nm, but φ decreases by 5% [see Table 3 in ref. (29)]. The spraying of a silver-doped soot coating yielded more oxidized (~6 at.%) and "crumpled" nanostructures, whereas the processing of a paper napkin with rapeseed oil soot, cyanoacrylate glue and fluorocarbon emulsion resulted in a 160 μm thick, non-wettable coating with a highly filamentous and macroporous (~0.5–1 mm) structure (25).

The differences in soot features predetermine the mechanisms of thermal transport and heat transfer by governing phonon scattering and interfacial thermal conductivity (29), thereby dictating the degree of supercooling and the freezing temperature depression (26). Consequently, flash freezing and surface-mediated heat conduction may cooperatively suppress the growth of ice crystals and contribute to the safe cryostorage of spermatozoa – a driving force of this work.

Motility and curvilinear velocity (VCL) of the post-thaw human spermatozoa

It has recently been hypothesized that the partial immersion of soot fabric-coated cryoboxes in liquid nitrogen leads to quasivitrification of the semen, induced by the availability of more ice nuclei and fewer ice crystals, ensuring survival rates above 70%, even when using mixtures of multicomponent cryoprotectants (27). Figures 4 and 5 address how the surface profile of soot coatings influences the success rate of cryopreservation when using flash freezing.

The observed dependencies are intriguing, since in contrast to slow freezing (26), here the variations in the average sperm motility from group-to-group are statistically insignificant with $p > 0.05$ (see the left chart in Fig. 4). This is attributed to the variation in quality among the

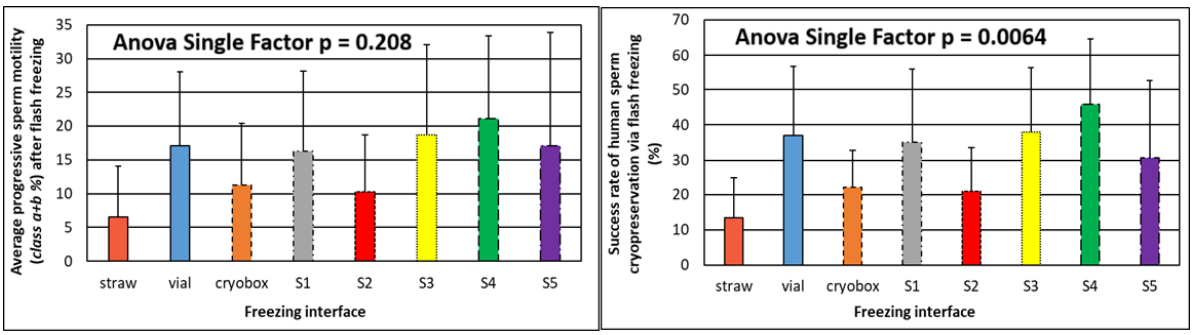


Figure 4. Average progressive sperm motility, *class a+b* (left chart), and cryostorage efficiency (right chart) after flash freezing/slow thawing using hydrophilic (straw, vial, cryobox) and superhydrophobic soot-coated surfaces. The high standard deviations observed in Figure 4 are consistent with the significant heterogeneity in the baseline semen quality of participants (ranging from normozoospermia to oligoasthenozoospermia). This leads to inherently high variability in cryotolerance and post-thaw vitality. The success rate is calculated as the ratio of post-thaw to pre-freeze progressive motility (*class a+b*), multiplied by 100.

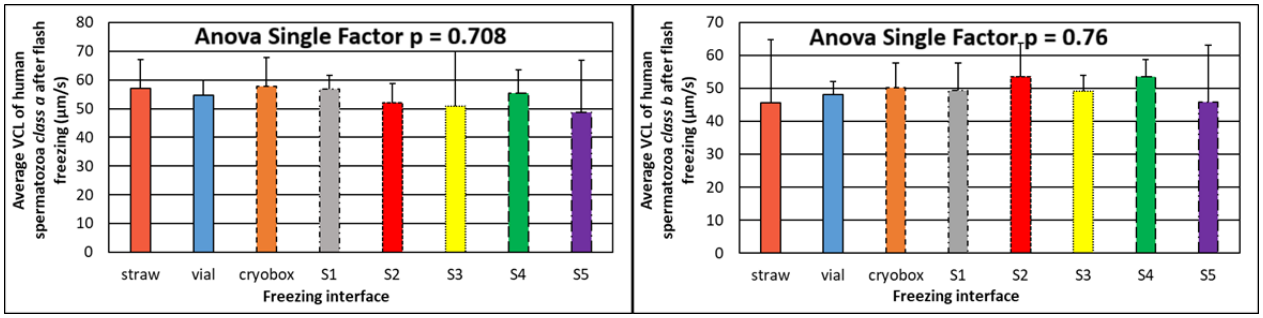


Figure 5. Average VCL of rapid progressive (*class a*, left) and medium progressive (*class b*, right) spermatozoa after flash freezing and slow thawing on hydrophilic (straw, vial, cryobox) and superhydrophobic soot-coated surfaces.

nine seminal fluids (e.g., viscosity, biochemical composition of the seminal plasma, initial sperm concentration and motility), in combination with the freezing technique and type of cryoprotectant used (see Discussion). These factors eliminated the positive impact of soot nanostructures reported previously (24, 25, 26, 27). Nevertheless, the soot-coated cryoboxes yield 5-15% more post-thaw forward-moving spermatozoa compared with the cryostraw and hydrophilic cryobox, making the difference in average success rates statistically significant (see the right chart in Fig. 4).

Another key finding is the higher percentage of post-thaw progressively motile gametes in the standard cryovial than in the ejaculates frozen using three out of five superhydrophobic cryoboxes. The former device contains a mixture of 400 µL semen-cryoprotectant, implying that sub-milliliter or milliliter seminal volumes, coupled with flash freezing, may benefit cryostorage and not injure the sperm due to non-uniform heat distribution in certain domains of the samples (30). Conversely, the cryostraw containing 100 µL liquid is characterized by the worst outcome among all freezing tools, suggesting that the overall surface area interacting with liquid nitrogen and transferring heat to the biological suspension must not be neglected. Consistent with the slow freezing protocol (26), the VCL of post-thaw cells is not substantially affected by the profile of the solid interface (see Fig. 5), falls within the requirements of the World Health Organization (~50-60 µm/s) and confirms our previous conclusion that the specific sperm cryopreservation techniques are less relevant to the motional capacity of thawed male gametes.

The higher quality of post-thaw ejaculate from the uncoated cryobox, compared with the soot fabric-coated cryobox ("cryobox" and "S2" in Fig. 4), is surprising and likely dictated by the different cooling rates, summarized in Figure 6.

The soot fabric-coated cryobox cools the semen at a rate ~2.6–3.3 times slower than all other cryoboxes. Therefore, the ejaculate remains in a metastable supercooled liquid state for more than 10 s (see the upper left chart in Fig. 6). This delays the extracellular ice formation (with respect to other cryoboxes) and blocks the outward movement of cell water, likely trigerring intracellular freezing and lethal end of spermatozoa (31). Such undesired supercooling effects are ascribed to the high thermal resistance of the solid interface (29), dominating the heat conduction upon direct

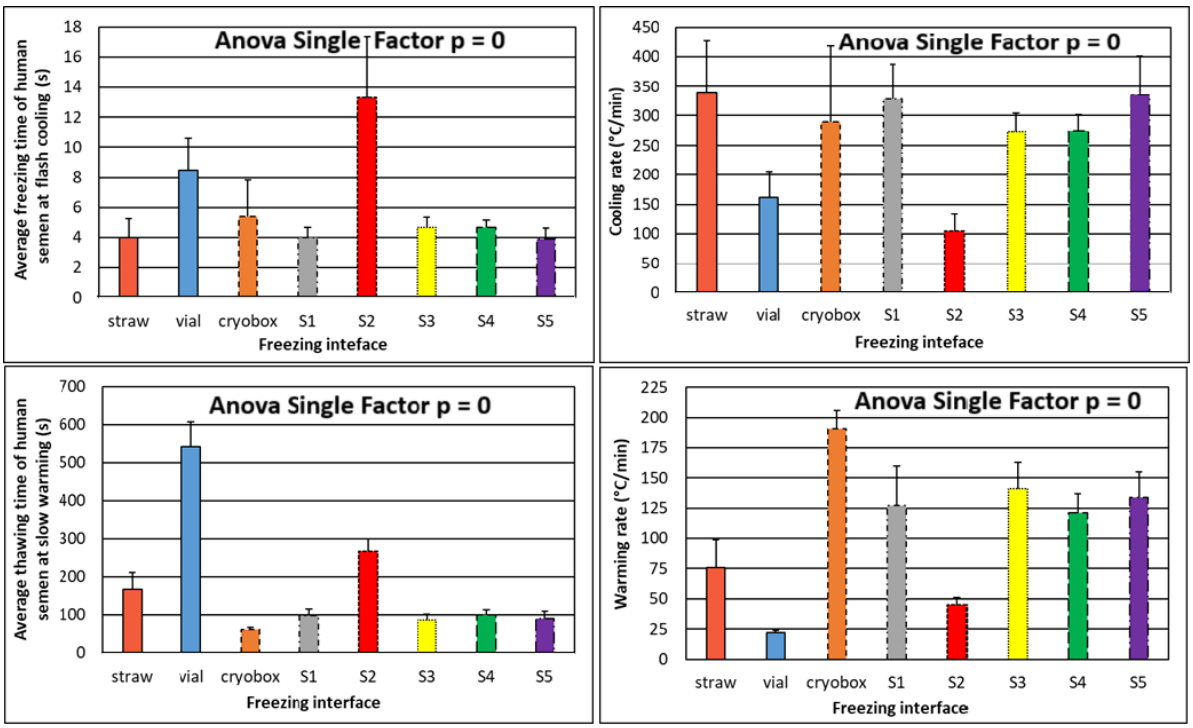


Figure 6. Average freezing-thawing times (left charts) and cooling-warming rates (right charts) of human semen during flash freezing and slow thawing using hydrophilic (straw, vial, cryobox) and superhydrophobic soot-coated surfaces. The cooling and warming rates are calculated as described in ref. (27).

contact with the coolant. When the heat flux is transferred to the seminal fluid via convection, due to the working principle of the cryogenic chamber intended to slow freezing, the differences in phonon scattering defined by the soot coatings are eliminated (26). The cooling and warming rates alone, though, are not conclusive. Comparison of the hydrophilic cryotools shows that the fastest cooling or warming (cryostraw; uncoated cryobox) actually leads to poorer outcome compared to the cryovial, where moderate cooling and slowest thawing provide ~5–10% higher sperm motility (see Figs 4 and 6). This is probably due to the volume and biochemistry of seminal plasmas, impacting the freezability of native semen (26, 32).

HEAD-TO-HEAD COMPARISON OF THE CURRENT RESULTS WITH PREVIOUS WORK

It is known that, ceteris paribus, the improperly calibrated freeze-thaw cycles are the main source of sperm cryoinjury (5, 6, 13, 14, 15, 19, 20, 21). From that viewpoint, the tendencies outlined above are extraordinary and imply that optimizing the interplay among sample volume, freezing tool geometry and wettability could suppress the intracellular ice formation and devitrification, offering a buffer against undesirable variations in cooling and warming rates. This is a compelling justification to conduct a detailed side-by-side analysis of the sperm vitality and motility after slow and flash freezing of the ejaculates of nine patients with the aid of Quinn's Advantage medium, as demonstrated in Figures 7 and 8.

While statistically insignificant, the small differences in column charts in Figure 7 suggest that slow freezing via carbon soot and Quinn's Advantage is slightly superior to flash freezing in terms of the percentage of forward-moving spermatozoa and overall success of cryostorage. Despite a two-order-of magnitude difference in freezing velocities, the average post-thaw motility and VCL for the hydrophilic cryovial or sample S4 are identical (see the left charts in Figs 7 and 8). Such a finding is extraordinary, since it undermines the generalizability of the two-factor freezing injury (14). To determine whether this outcome is an artifact of averaging, Table 1 presents the patient-specific success rates of cryopreservation.

In six of nine patients, some surface profiles and sperm volumes suppress the impact of the freezing technique, resulting in comparable survival rates and, in some individuals, an identical percentage of progressively motile spermatozoa (see Table 1 and Figs S6-S7-S9-S12-S14-S28-S30 in the SI). This parity holds true across multiple solid surface/sperm volume combinations within a single patient (see Patients 4 and 8 in Table 1), suggesting that the biochemistry of seminal plasma is a relevant factor mitigating the effect of the cooling regime. The similarity in mean kinematic parameters between the two experimental sets (see columns "*Initial a+b*" and "*Initial VCL*" in Figs 7 and 8) provides robust evidence that our findings are not merely accidental.

DISCUSSION

Although exciting, the outcome of this research (average survival rate of *class a+b* = 35.4%, according to the numbers for flash freezing in Table 1) appears worse than those obtained via other sperm cryopreservation approaches (19, 20, 21), where this indicator ranges within 69–79% (note, these values reflect the total motility *a+b+c*). This may elicit skepticism within the scientific community regarding the added value of using hydrophobic soot wastes for the fabrication of extremely water-repellent cryopreservation tools.

This ostensibly negative result can be interpreted by examining the biochemical composition of Quinn's Advantage medium. According to the product's data sheets, it is a commercial cryoprotectant composed mainly of glycerol and pharmaceutical ingredients including gentamicin, human serum albumin (HSA), sodium chloride, etc. Its formulation excludes carbohydrates, such as sucrose and raffinose, available in other similar cryoprotectants SpermFreeze™ (FertiPro, Belgium) and CryoSperm™ (CooperSurgical, USA) (27).

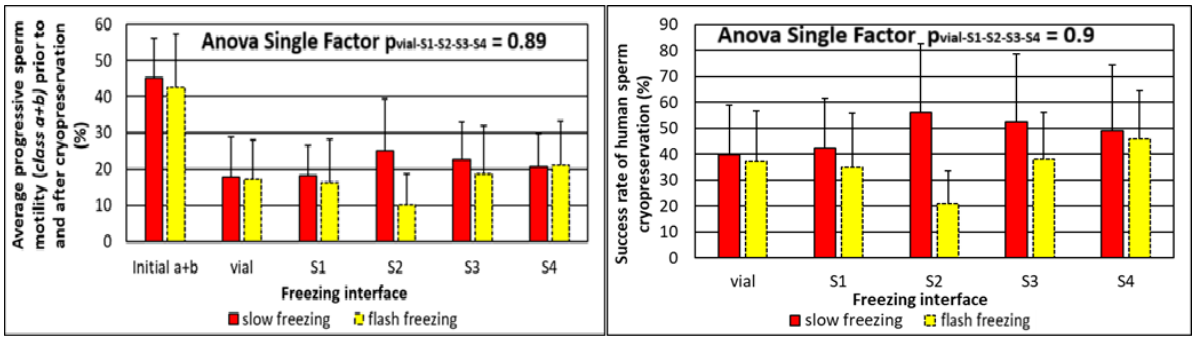


Figure 7. Comparison of the average progressive sperm motility *class a+b* (left chart) and success rate after slow and flash freezing (right chart) of the semen of nine patients via Quinn's Advantage medium. Sample S5 is different in both studies and therefore it is excluded from the analysis. The column charts concerning slow freezing are built upon the data from ref. (26), published as an open access article under CC BY-NC-ND 4.0 license.

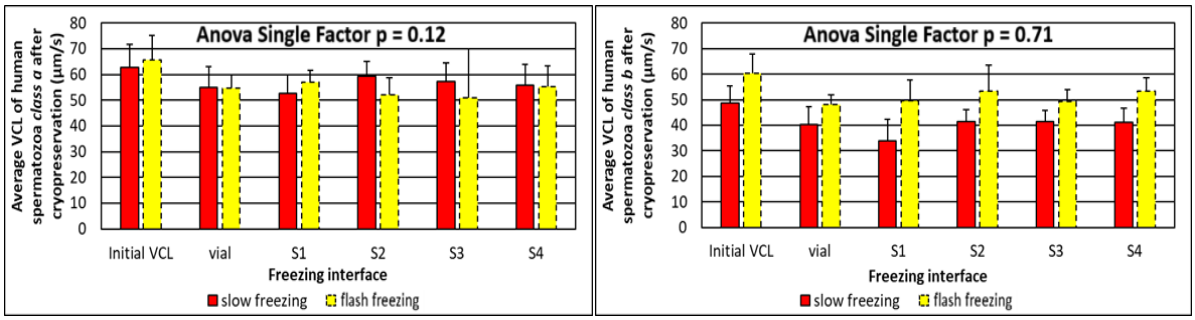


Figure 8. Comparison of the average VCL of rapid progressive (*class a*, left) and medium progressive (*class b*, right) spermatozoa after slow and flash freezing of the semen of nine patients via Quinn's Advantage medium. Sample S5 is different in both studies and therefore it is excluded from the analysis. The column charts concerning the slow freezing are built upon the data from ref. (26), published as an open access article under CC BY-NC-ND 4.0 license.

Table 1. Success rate after slow and flash freezing of the ejaculates of nine patients (post-thaw to pre-freeze progressive motility, multiplied by 100. **Bold data** indicate >70% post-thaw progressively motile spermatozoa, while <u>underlined data</u> denote comparable post-thaw motility percentage. The authenticity of these data is confirmed by thirty snapshot images, included as Figures S1-S30 in the supporting information.

Patient	Success rate of human sperm cryopreservation (%) after slow freezing (SL) and flash freezing (IF) via Quinn's Advantage Sperm Freezing Medium																	
	1		2		3		4		5		6		7		8		9	
	SL	IF	SL	IF	SL	IF	SL	IF	SL	IF	SL	IF	SL	IF	SL	IF	SL	IF
vial_300–400 µL	30	14	**82**	43	13	**79**	<u>34</u>	<u>32</u>	<u>23</u>	<u>23</u>	50	27	<u>54</u>	<u>51</u>	43	17	29	49
S1	36	5	36	49	9	**74**	61	41	36	9	45	24	**76**	49	<u>24</u>	<u>22</u>	58	42
S2	31	5	**98**	36	23	37	69	14	40	5	55	27	**84**	32	23	7	**81**	26
S3	25	14	70	43	<u>23</u>	<u>33</u>	24	45	47	2	**86**	39	**100**	59	<u>41</u>	<u>50</u>	<u>54</u>	<u>58</u>
S4	31	21	59	37	17	**74**	<u>39</u>	<u>46</u>	46	23	**82**	45	**100**	58	<u>34</u>	<u>32</u>	31	**75**

Given the cryoprotective function of proteins and sugars, HSA binds to the hydrophilic phospholipid heads of the lipid bilayer, serving as a chain-breaking antioxidant stopping lipid peroxidation (18, 31). By increasing the concentration of extracellular solutes, sugars create an osmotic gradient, accelerate cell dehydration and equilibrate the osmotic pressure altered by permeable cryoprotectants (33). Therefore, the insufficient efficacy of Quinn's Advantage medium and soot-coated cryoboxes during flash freezing is due to the lack of carbohydrates and the supercooling of seminal fluids, hindering the timely removal of cell water and triggering intracellular icing. This novel insight is crucial, as it enables the customization of cryoprotocols based on available cryoprotectant and cryogenic infrastructure, allowing for accurate prediction of outcomes. If one has the expertise or facilities for flash freezing, commercial cryoformulations should contain sugars and proteins, which when integrated with superhydrophobic soot coatings ensure survival rates within 74–100% (27). Alternatively, if slow freezing is the only feasible option for sperm cryostorage, Quinn's Advantage (or an identical cryoprotectant) is recommended. It supports osmotic balance and avoids premature cytoplasmic dehydration and hypertonic damage (15), while being capable of providing (sometimes) exceptional post-thaw progressive motility of 80-100% (26). The credibility of this new knowledge discussed in the preceding sentences is upheld by the low efficiency of soot-mediated slow freezing when utilizing SpermFreeze™ containing 1-5% sucrose [see Fig. 2a in ref. (35)]. Since Quinn's Advantage™, SpermFreeze™ and CryoSperm™ are standard commercial freezing media (27), our results will be useful to both the scientific community and industry (reproductive health centers).

Along with the composition of cryoprotectants, the physicochemical profile of the soot is the second determinative element in sperm cryopreservation, since it mediates the freezing process by modulating (hastening or delaying) heat conduction at the solid-liquid interface and governing osmotic equilibrium. For instance, silver-doped soot (S1) and alcohol-flurocarbon-modified quasisquare soot (S3) appear to be good candidates for flash freezing, even when utilizing Quinn's Advantage, due to the higher density of ice-active sites or lower porosity compared to other carbon nanostructures (25, 29). Soot fabrics (S2) supplemented with this type of cryoprotectant are certainly a much better choice for slow cooling applications (see Table 1). Ultimately, optimizing sperm cryostorage is achievable by matching the properties of rapeseed oil soot and freezing extenders with the engineering approach, where slow-heat-transfer coatings should be applied to optimize slow freezing without sugars, while samples ensuring moderate heat retardation are suitable for flash freezing with non-permeable cryoformulations.

The above discussion fails to explain adequately the underlying mechanism behind the similar survival rates and percentage of progressively motile gametes among distinct patients, regardless of the freezing method, interfacial characteristics and seminal volume. Examining the time-temperature diagram for ice nucleation and crystal growth reveals that achieving a glass transition requires cooling rates of ~18 000 °C/min (34). This rate is unattainable with our experimental setup, especially via the non-wettable soot-coated surfaces (see the upper right chart of Fig. 6). We propose that the key physical factor during soot-mediated sperm cryopreservation is the absence of an ice-water front, leading to a spherical apex of the seminal droplet (35) and indicating that the solid-liquid phase transitions proceed without significant changes in the ratio of ice-water mass densities (36). Instead of growing into large crystals, early-stage ice nuclei in the ejaculates form a few scattered ice bridges, leaving large amorphous (non-crystalline, quasi-liquid) areas between ice grains. This maintains chemical equilibrium in some regions of the biological suspension independently of the cooling rates, resulting in similar post-thaw survival. Although tentative, our interpretation is substantiated by the fact that both methods produce gray-colored sperm droplets in the first freezing phase outside the styrofoam chamber, contrasting with the final milky-like color of the semen [see Fig. 5 in ref. (26), Fig. 9 in ref (27) and Fig. 1 in this article]. Large ejaculate volume significantly impacts the cryoinjury by controlling the physical spacing of ice crystals. Because ice nucleation is a stochastic process (37), crystals form unevenly, allowing for local adjustment of solute concentration and justifying the good success rates using hydrophilic cryovials (up to 79-82%, according to Table 1).

CONCLUSIONS

The rapid cooling of native human ejaculates mixed 1:1 v/v with Quinn's Advantage Sperm Freezing Medium, using extremely water-repellent soot-coated cryoboxes and three reference freezing instruments (cryostraw, cryovial and an uncoated cryobox), revealed that unlike slow freezing, the hydrophilic interface combined with larger seminal volumes favors the recovery of sperm vitality and motility. This interesting result was primarily attributed to increased physical distance between individual ice grains, forming randomly in the cellular suspension, thus regulating salt buildup. A second decisive factor was the impeded exosmosis and probable occurrence of intracellular icing, caused by the supercooling effects of superhydrophobic soot coatings and the lack of sugars in the chosen cryoprotectant. Nonetheless, carbon nanostructures maintained the semen in a quasi-liquid state, confirmed by the spherical freezing cap and absence of a sharp ice-water front (35, 36), leading to sperm survival rates on par with slow cooling. This infers that the two-factor freezing injury may not be a universal mechanism and is potentially avoidable by selecting custom equipment and adjusting liquid volumes – a pivotal opportunity to redefine the boundaries of contemporary cryobiology.

Acknowledgments: This research was performed thanks to the financial support of Bulgarian National Science Fund under grant № KP-06-H57/1/15.11.2021.

Supplementary data is available on the CryoLetters website (www.cryoletters.org)

REFERENCES

1. Hughes G & Martins da Silva S (2023) *Reprod. Fertil.* **4**, e220106. DOI: https://doi.org/10.1530/RAF-22-0106
2. Huang B, Wang Z, Kong Y, Jin M & Ma L (2023) *BMC Public Health* **23**, 2195. DOI: https://doi.org/10.1186/s12889-023-16793-3
3. Chen H, Lin R, Wu Z, Zhou H, Wang C, Gan X, Xu K, Sun K, Deng X & Shu J (2023) *Cryobiology* **112**, 104554. DOI: https://doi.org/10.1016/j.cryobiol.2023.104554
4. Safian F, Novin M G, Nazarian H, Mofarahe ZS, Abdollahifar MA, Jajarmi V, Karimi S, Kazemi M, Chien S & Bayat M (2021) *Cryobiology* **98**, 239-244. DOI: http://doi.org/10.1016/j.cryobiol.2020.09.005
5. Ozimic S, Ban-Frangez H & Stimpfel M (2023) *Curr. Issues Molecular Biol*. **45**, 4716-4734. DOI: https://doi.org/10.3390/cimb45060300
6. Podgrajsek R, Bohla L, Pungert T, Pizem J, Jazbec K, Malicev E & Stimpfel M (2024) *Int. J. Molecular Sci*. **25**, 4157. DOI: https://doi.org/10.3390/ijms25084157
7. Yu M, Marquez-Curtis LA & Elliott JAW (2024) *Cryobiology* **115**, 104857. DOI: http://doi.org/10.1016/j.cryobiol.2024.104857
8. Eskandari A, Leow TC, Rahman MBA & Oslan SN (2020) *Biomolecules* **10**, 1649. DOI: https://doi.org/10.3390/biom10121649
9. Gruneberg AK, Graham LA, Eves R, Agrawal P, Oleschuk RD & Davies PL (2021) *Cryobiology* **99**, 28-39. DOI: https://doi.org/10.1016/j.cryobiol.2021.01.017
10. Mazur P (1984) *Am. J. Physiol*. **247**, C125-C142. DOI: https://doi.org/10.1152/ajpcell.1984.247.3.C125
11. Lin M, Cao H & Li J (2023) *Acta Biomater*. **155**, 35-56. DOI: http://doi.org/10.1016/j.actbio.2022.10.056
12. Pegg DE (2020) *Cryobiology* **93**, 3-11. DOI: http://doi.org/10.1016/j.cryobiol.2020.01.005
13. Morris GJ, Acton E, Murray BJ & Fonseca F (2012) *Cryobiology* **64**, 71-80. DOI: http://doi.org/10.1016/j.cryobiol.2011.12.002
14. Mazur P, Leibo SP & Chu EHY (1972) *Exp. Cell. Res*. **71**, 345-355. DOI: http://doi.org/10.1016/0014-4827(72)90303-5
15. Sieme H, Oldenhof H & Wolkers WF (2016) *Animal Rep. Sci*. **169**, 2-5. DOI: https://doi.org/10.1016/j.anireprosci.2016.02.004
16. Pegg DE & Diaper MP (1988) *Biophys. J.* **54**, 471-488. DOI: https://doi.org/10.1016/S0006-3495(88)82980-1
17. Landecker H (2024) *BioSoc*. **19**, 635-655. DOI: https://doi.org/10.1057/s41292-024-00331-4

18. Fleming SD & Thomson LK (2025) *Antioxidants* **14**, 402. DOI: https://doi.org/10.3390/antiox14040402
19. Liu J, Tanrikut C, Wright DL, Lee GY, Toner M, Biggers JD & Toth TL (2016) *Cryobiology* **73**, 162-167. DOI: http://doi.org/10.1016/j.cryobiol.2016.08.004
20. Huang C, Gan RX, Zhang H, Zhou WJ, Huang ZH, Jiang SH, Ji XR, Gong F, Fan LQ & Zhu WB (2020) *Fertil. Steril*. **114**, 301-310. DOI: https://doi.org/10.1016/j.fertnstert.2020.03.032
21. Petrushko M, Yurchuk T, Todorov P, Hristova E, Piniaiev V, Isachenko E, Rahimi G, Mallmann P & Isachenko V (2021) *Cryobiology* **103**, 39-44. DOI: http://doi.org/10.1016/j.cryobiol.2021.09.013
22. Baharsaadi M, Hezavehei M, Shahverdi A & Halvaei I (2024) *Cryobiology* **114**, 104840. DOI: http://doi.org/10.1016/j.cryobiol.2023.104840
23. Li L, Tian Y, Li Z, Duan P, Wang X, Chen S, Wang L *et.al*. (2023) *Cryobiology* **112**, 104555. DOI: http://doi.org/10.1016/j.cryobiol.2023.104555
24. Esmeryan KD, Stamenov GS & Chaushev TA (2020) *Cryobiology* **92**, 263-266. DOI: http://doi.org/10.1016/j.cryobiol.2019.10.004
25. Esmeryan KD, Fedchenko YI, Gyoshev SD, Lazarov Y, Chaushev TA & Grakov T (2022) *ACS Appl. Bio Mater*. **5**, 3519-3529. DOI: https://doi.org/10.1021/acsabm.2c00457
26. Esmeryan KD & Chaushev TA (2024) *Cryobiology* **115**, 104863. DOI: https://doi.org/10.1016/j.cryobiol.2024.104863
27. Esmeryan KD, Fedchenko YI & Chaushev TA (2025) *Cryobiology* **118**, 105195. DOI: http://doi.org/10.1016/j.cryobiol.2025.105195
28. Xu L, Wan G, Sun L & Lin L (2024) *Fuel* **365**, 131175. DOI: https://doi.org/10.1016/j.fuel.2024.131175
29. Esmeryan KD, Grakov T, Vergov LG, Lazarov Y, Fedchenko Y & Staykov S (2023) *Appl. Thermal Eng*. **219**, 119590. DOI: http://doi.org/10.1016/j.applthermaleng.2022.119590
30. Kilbride P, Lamb S, Milne S, Gibbons S, Erro E, Bundy J, Selden C, Fuller B & Morris J (2016) *Cryobiology* **73**, 47-54. DOI: http://doi.org/10.1016/j.cryobiol.2016.05.013
31. Murray KA & Gibson MI (2022) *Nat. Rev. Chem*. **6**, 579-593. DOI: http://doi.org/10.1038/s41570-022-00407-4
32. Esmeryan KD & Chaushev TA (2026) *Cryoletters* **47**, 120-125. DOI: https://doi.org/10.54680/fr26210110212
33. Isachenko V, Rahimi G, Mallmann P, Sanchez R & Isachenko E (2017) *Andrology* **5**, 1055-1063. DOI: https://doi.org/10.1111/andr.12414
34. Pegg D 2005 *Hum. Fert*. **8**, 231-239. DOI: https://doi.org/10.1080/14647270500054803
35. Esmeryan KD, Paneva MM, Panev PP & Chaushev TA (2025) *Colloid J*. **87**, 255-267. DOI: https://doi.org/10.1134/S1061933X24601288
36. Dai Z, Xu J, Wang Z, Wu W, Wang Y & Liu Y (2026) *Appl. Phys. Lett*. **128**, 032702. DOI: https://doi.org/10.1063/5.0306980
37. Deck LT, Ochsenbein DR & Mazzotti M (2022) *Int. J. Pharma*. **625**, 122051. DOI: http://doi.org/10.1016/j.ijpharm.2022.122051